Aerosol Composition and Sources during the Chinese Spring Festival: Fireworks, Secondary Aerosol, and Holiday Effects

Qi Jiang[1,3], Yele Sun[1,2*], Zifa Wang[1], Yan Yin[2,3]

[1]State Key Laboratory of Atmospheric Boundary Layer Physics and Atmospheric Chemistry, Institute of Atmospheric Physics, Chinese Academy of Sciences, Beijing 100029, China

[2]Collaborative Innovation Center on Forecast and Evaluation of Meteorological Disasters, Nanjing University of Information Science & Technology, Nanjing, 210044, China

[3]Key Laboratory for Aerosol-Cloud-Precipitation of China Meteorological Administration, Nanjing University of Information Science & Technology, Nanjing 210044, China

Correspondence to: sunyele@mail.iap.ac.cn

Abstract

Aerosol particles were characterized by an Aerodyne Aerosol Chemical Speciation Monitor (ACSM) along with various collocated instruments in Beijing, China to investigate the aerosol composition and sources during the Chinese Spring Festival, 2013. Three fireworks (FW) events exerting significant and short-term impacts on fine particles ($PM_{2.5}$) were observed on the days of Lunar New Year, Lunar Fifth Day, and Lantern Festival. The FW showed major impacts on non-refractory potassium, chloride, sulfate, and organics in PM_1, of which the FW organics appeared to be mainly secondary with its mass spectrum resembling to that of secondary organic aerosol (SOA). Pollution events (PEs) and clean periods (CPs) alternated routinely throughout the study. Secondary particulate matter (SPM = SOA + sulfate + nitrate + ammonium) dominated PM_1 accounting for 63-82% during the nine PEs observed. The elevated contributions of secondary species during PEs resulted in a higher mass extinction efficiency of PM_1 (6.4 $m^2 g^{-1}$) than that during CPs (4.4 $m^2 g^{-1}$). The Chinese Spring Festival also provides a unique opportunity to study the impacts of reduced anthropogenic emissions on aerosol chemistry in the city. The primary species showed ubiquitous reductions during the holiday period with the largest reduction for cooking OA (69%), nitrogen monoxide (54%), and coal combustion OA (28%). The secondary sulfate, however, remained minor change, and the SOA and the total $PM_{2.5}$ even slightly increased. These results have significant implications that controlling local primary source emissions, e.g., cooking and traffic activities, might have limited effects on improving air quality during PEs when SPM that is formed over regional scales dominates aerosol particle composition.

1 Introduction

Air pollution caused by fine particles ($PM_{2.5}$) is of great concern in densely populated megacities because of its adverse effects on human health and regional air quality (Molina and Molina, 2004;Chan and Yao, 2008). The health risk of air pollution is greater than expected leading to around 7 million people's death in 2012 according to the latest report by World Health Organization (http://www.who.int/mediacentre/news/releases/2014/air-pollution/en/). The Beijing metropolitan area is one of the most populous megacities in the world with the population reaching 20.69 million by the end of 2012 (Beijing Municipal Bureau of Statistics). According to Beijing Municipal Environmental Protection Bureau, the annual average concentration of $PM_{2.5}$ was 89.5 μg m^{-3} in 2013, about 2.5 times the National Ambient Air Quality Standards of China (35 μg m^{-3} for annual average), which indicates severe fine particle pollution in Beijing. As a result, extensive studies have been made recently to investigate the sources of $PM_{2.5}$. The results showed that secondary inorganic aerosol (SIA = sulfate + nitrate + ammonium), coal combustion, traffic emissions (gasoline and diesel), biomass burning, cooking emissions and dust are the major sources of $PM_{2.5}$ (Zheng et al., 2005;Song et al., 2006;Zhang et al., 2013), and the source contributions varied significantly among different seasons. Despite this, improving air quality in Beijing remains a great challenge due to the very complex sources and dynamic evolution processes of aerosol particles.

Fine particles from various source emissions can be either primary from direct emissions, e.g., fossil fuel combustion and biomass burning, or secondary from atmospheric oxidation of gas-phase species. The fireworks (FW) is one of the most important primary source that can exert significant and short-time impacts on air

quality. The fireworks burning emits a large amount of gaseous pollutants, e.g., sulfur dioxide (SO_2) and nitrogen oxide (NO_x) (Vecchi et al., 2008;Huang et al., 2012), and also fine particles comprising organic/elemental carbon, sulfate, potassium, chloride and various metals, e.g., copper (Cu), barium (Ba), strontium (Sr) and magnesium (Mg) (Moreno et al., 2007;Wang et al., 2007;Li et al., 2013). The enhanced short-term air pollution by fireworks can substantially increase health risk levels (Godri et al., 2010;Yang et al., 2014) and reduce visibility for hours (Vecchi et al., 2008). However, previous studies on chemical characterization of fireworks in China were mostly based on filter measurements with a time resolution of 12 h or 24 h (Wang et al., 2007;Zhang et al., 2010;Feng et al., 2012;Huang et al., 2012;Cheng et al., 2014;Zhao et al., 2014), which may have large uncertainties in accurate quantification of chemical composition of FW particles. Drewnick et al. (2006) first conducted real-time size-resolved chemical composition measurements during the New Year's period in Mainz, Germany using an Aerodyne Time-of-Flight Aerosol Mass Spectrometer (ToF-AMS). To our knowledge, there are no such real-time measurements of chemical composition of aerosol particles during fireworks events in China yet, which limits our understanding on the rapid formation and evolution of fireworks events, and also their impacts on air pollution.

Secondary aerosol is of more concern compared to primary aerosol because it is formed over regional scales and exerts impacts on air quality over wider areas. Therefore, extensive studies have been conducted in recent years to characterize the sources and formation mechanisms of secondary aerosol (Yao et al., 2002;Duan et al., 2006;Sun et al., 2006;Wang et al., 2006;Guo et al., 2010;Yang et al., 2011;Sun et al., 2013b;Zhang et al., 2013;Zhao et al., 2013). SIA was observed to contribute a large

fraction of $PM_{2.5}$ and played an enhanced role during haze episodes due to the faster heterogeneous reactions associated with higher humidity. While SIA was relatively well characterized, secondary organic aerosol (SOA) is poorly understood. The recent deployments of Aerodyne Aerosol Mass Spectrometers (AMS) greatly improved our understanding on sources and evolution processes of organic aerosol (OA) in China, and also primary organic aerosol (POA) and SOA by positive matrix factorization (PMF) of organic mass spectra (Huang et al., 2010;Sun et al., 2010;He et al., 2011;Sun et al., 2012;Sun et al., 2013b;Zhang et al., 2014). SOA was found to play different roles among different seasons. While SOA is more significant in summer (Huang et al., 2010;Sun et al., 2010;Sun et al., 2012), POA generally plays a more important role during wintertime (Sun et al., 2013b). Despite this, the role of SOA in fine particle pollution in Beijing is not well known, in particular during wintertime, a season with frequent occurrences of pollution episodes (Sun et al., 2013b;Zhang et al., 2014). Of particular interest, this study took place in the month with the most important holiday in China, i.e., the Spring Festival. The source emissions (e.g., traffic and cooking) had significant changes due to a large reduction of population and anthropogenic activities in the city. This provides a unique opportunity to investigate how source changes affect aerosol chemistry including primary emissions and secondary formation in Beijing. Although Huang et al. (2012) investigated such a holiday effect on aerosol composition and optical properties in Shanghai, the data analyses were limited by daily average composition measurements and also the significantly different meteorological conditions between holiday and non-holiday periods.

In this study, an Aerosol Chemical Speciation Monitor (ACSM) along with

various collocated instruments was deployed in Beijing during February 2013. The chemical composition of PM_1 from fireworks is first quantified in Beijing based on the high time resolution measurements of non-refractory submicron aerosol species (organics, sulfate, nitrate, ammonium, chloride, and potassium) and black carbon. The impact of fireworks on PM pollution during Chinese Lunar New Year (LNY), Lunar Fifth Day (LFD), and Lantern Festival (LF) are investigated, and the roles of secondary formation in PM pollution are elucidated. Further, the impacts of reduced anthropogenic emissions during the holiday on primary and secondary aerosols in the city are illustrated, which has significant implications for making air pollution control strategies in Beijing.

2 Experimental

2.1 Sampling site

The measurements in this study were conducted at the Institute of Atmospheric Physics (IAP), Chinese Academy of Sciences (39°58'28''N, 116°22'16"E), an urban site located between the north third and fourth ring road in Beijing (Sun et al., 2012). Aerosol characterization was performed from 1 February to 1 March 2013, during which three episodes with significant influences of fireworks, i.e., Lunar New Year (LNY), Lunar Fifth Day (LFD), and Lantern Festival (LF), were observed (Fig. 1). The meteorological conditions during the measurement period are reported in Fig. 1. Winds at the ground surface were generally below 2 m s^{-1} and temperature averaged 0.6 °C. Relative humidity (RH) varied periodically with higher values generally associated with higher particulate matter (PM) pollution.

2.2 Aerosol sampling

The chemical composition of non-refractory submicron aerosol particles (NR-PM_1) including organics, sulfate, nitrate, ammonium, and chloride were measured on-line by an Aerodyne Aerosol Chemical Speciation Monitor (ACSM) at an approximate 15-min time intervals (Ng et al., 2011b). The ACSM was built upon previous versions of AMS (Jayne et al., 2000;DeCarlo et al., 2006). However, the ACSM has no size information and also a lower sensitivity and lower mass resolution due to the use of a commercial-grade quadrupole mass analyzer (Ng et al., 2011b). The advantage of the ACSM is its robustness for long-term and routine aerosol particle composition measurements. A two-wavelength Aethalometer (Model AE22, Magee Scientific Corp.) was used to measure refractory black carbon (BC) that the ACSM cannot detect.

The light extinction of dry fine particles (b_{ext}, M m^{-1}, 630 nm) was measured by a Cavity Attenuated Phase Shift Spectrometer particle extinction monitor, CAPS PM_{ex} (Massoli et al., 2010). The CAPS PM_{ex} was measured at 1 s time resolution with a precision (3 σ) of 1 M m^{-1}. The mass concentration of $PM_{2.5}$ was determined by a heated Tapered Element Oscillating Microbalance, TEOM, and the collocated gaseous species (including CO, SO_2, NO, NO_x and O_3) were measured by various gas analyzers (Thermo Scientific) at 1 min time resolution. The detailed descriptions of aerosol and gas measurements were given in Sun et al. (2013b).

2.3 ACSM data analysis

The ACSM data were analyzed for the mass concentrations and chemical composition of NR-PM_1 using standard ACSM software (v 1.5.3.2) written within Igor Pro (WaveMetrics, Inc., Oregon USA). A composition-dependent collection efficiency (CE) recommended by Middlebrook et al.(2012), CE = max (0.45, 0.0833

160 + 0.9167 × ANMF), was used to account for the incomplete detection due to the
161 particle bouncing effects (Matthew et al., 2008) and the influences caused by high
162 mass fraction of ammonium nitrate (ANMF). The default relative ionization
163 efficiencies (RIEs) were used in this study, except ammonium (RIE = 6.5) that was
164 determined from IE calibration.

165 Quantification of K^+ is challenging for ACSM because of a large interference of
166 organic $C_3H_3^+$ at *m/z* 39 and also uncertainties caused by surface ionization (Slowik et
167 al., 2010). In this work, we found that *m/z* 39 was tightly correlated with *m/z* 43 that is
168 completely organics during non-fireworks (NFW) periods ($r^2 = 0.87$, slope = 0.45, Fig.
169 S1). However, higher ratios of *m/z* 39/43 during FW periods were observed due to the
170 elevated K^+ signal from burning of fireworks. Assuming that *m/z* 39 was primarily
171 contributed by organics during NFW periods, the excess *m/z* 39 signal, i.e., K^+, can
172 then be estimated as *m/z* 39 – *m/z* 43 × 0.45. The $^{41}K^+$ (*m/z* 41) was calculated using
173 its isotopic ratio of 0.0722, i.e., $^{41}K^+ = 0.0722 \times K^+$. The K^+ signal was converted to
174 mass concentration with a RIE of 2.9 that was reported by Drewnick et al. (2006). The
175 KCl^+ (*m/z* 74) and $^{41}KCl^+/K^{37}Cl^+$ (*m/z* 76) were estimated by the differences between
176 the measured and PMF modeled *m/z* 74 (see Fig. S2 for details). Not surprisingly, the
177 quantified KCl^+ highly correlates with K^+ ($r^2 = 0.82$). The chloride concentration was
178 also biased at *m/z* 35 during some periods (e.g., LNY, Fig. S3), which is likely due to
179 the interferences of NaCl from fireworks. Therefore, Cl^+ (*m/z* 35) was recalculated
180 based on its correlation with *m/z* 36 (mainly HCl^+ with negligible C_3^+ and ^{36}Ar), i.e.,
181 *m/z* 35 = 0.15 × *m/z* 36, and $^{37}Cl^+$ was calculated using an isotopic ratio of 0.323, i.e.,
182 $^{37}Cl^+ = 0.323 \times ^{35}Cl^+$. A comparison of the time series of default and recalculated
183 chloride is shown in Fig. S3b.

The positive matrix factorization (PMF) with the algorithm of PMF2.exe in robust mode (Paatero and Tapper, 1994) was performed on organic aerosol (OA) mass spectra (*m/z* 12 – 120) to resolve distinct OA components from different sources. The PMF results were evaluated with an Igor Pro-based PMF Evaluation Tool (PET, v 2.04) (Ulbrich et al., 2009) following the procedures detailed in Zhang et al. (2011). After a careful evaluation of the spectral profiles, diurnal variations and correlations with external tracers, a 6-factor solution with rotational forcing parameter fpeak = -1 (Q/Q_{exp} = 4.3) was chosen, yielding a hydrocarbon-like OA (HOA), a cooking OA (COA), a coal combustion OA (CCOA), and three oxygenated OA (OOA) components, which were recombined into one OOA component. The four OA components show very similar mass spectral profiles (r^2 = 0.86 – 0.99) and diurnal variations (Fig. S4) to those observed during winter 2011-2012 (Sun et al., 2013b). A detailed summary of key diagnostic plots of the PMF solution are given in Fig. S5 – Fig. S8.

3 Results and discussion

3.1 Identification and quantification of fireworks events

Burning of fireworks has been found to emit a large amount of K^+, which can be used to identify the FW events (Drewnick et al., 2006;Wang et al., 2007). As shown in Fig. 1 and Fig. S9, three FW events with significantly elevated K^+ were observed on the days of Lunar New Year (LNY, 9-10 February), Lunar Fifth Day (LFD, 14 February), and Lantern Festival (LF, 24 February), respectively. All three FW events started approximately at 18:00 and ended at midnight except LNY with a continuous FW impact until 4:00 on the second day. Fig. 1 shows that the relative humidity was generally below 30% during LNY and LFD. While the wind speed at the ground

surface remained consistently below 2 m s^{-1}, it was increased to ~ 4 m s^{-1} at the height of 100 m. Also note that there was a wind direction change in the middle of the two events. The meteorological conditions during LF were stagnant with wind speed generally below 2 m s^{-1} across different heights. The relative humidity was ~50% and the temperature averaged 3.5°C.

To estimate the contributions of fireworks, we first assume that the background concentration of each species has a linear variation during FW period. A linear fit is then performed on the 6 h data before and after FW events. The difference between the measured and the fitted value is then assumed as the contribution from FW. The typical examples for estimating FW contributions are shown in Fig. S10. It should be noted that this approach might significantly overestimate the FW contributions of primary species (e.g., HOA, COA, CCOA, and BC) that were largely enhanced during the typical FW periods (18:00 – 24:00) due to the increased local emissions (see Fig. S11 for diurnal variations). However, it should have a minor impact on secondary species (e.g., SO_4^{2-}, NO_3-, and OOA) because of their relatively stable variations between 18:00-24:00. As shown in Fig. 1, all aerosol species showed substantial increases from 15:00 to 21:00 on the day of LNY which coincidently corresponded to a gradual change of wind direction. Therefore, regional transport might have played dominant roles for the evolution of chemical species during this period. For these reasons, only the FW contributions between 23:30, 9 February and 3:30, 10 February when the meteorological conditions were stable were estimated. The FW contributions during LFD might also be overestimated due to the influences of regional transport as suggested by the wind direction change in the middle.

Considering above, the contributions estimated in this work would represent the upper limits of FW.

3.2 Mass concentration and chemical composition of FW aerosols

Figure 1 shows the time series of mass concentrations of PM_1, $PM_{2.5}$, and submicron aerosol species from 1 February to 1 March 2013. Because ACSM cannot measure the metals (e.g., Sr, Ba, Mg, etc.) that were significantly enhanced during FW periods (Wang et al., 2007;Vecchi et al., 2008) , the PM_1 in this study refer to NR-PM_1 (= Org + SO_4^{2-} + NO_3^- + NH_4^+ + Chl+ K^+ + KCl) + BC. The $PM_{2.5}$ showed three prominent FW peaks with the maximum concentration occurring at ~00:30 during LNY and ~21:30 during LFD and LF, respectively. The peak concentration of $PM_{2.5}$ during LNY is more than 10 times higher than the China National Ambient Air Quality Standard (75 μg m^{-3}, 24 h average). The average FW-$PM_{2.5}$ mass concentrations during three FW events all exceeded 100 μg m^{-3}. These results suggest that fireworks have large impacts on fine particle pollution, yet generally less than half day (approximately 10 h for LNY, and 6 h for LFD and LF). The PM_1 also showed increases during the FW periods, yet not as significant as $PM_{2.5}$. In fact the correlation of PM_1 versus $PM_{2.5}$ shows much lower $PM_1/PM_{2.5}$ (0.08 – 0.19) ratios during three FW events than that observed during NFW periods (0.90) (Fig. 2). One of the reasons is likely due to the mineral dust component and metals from fireworks that ACSM did not measure. However, the metals that were largely enhanced during FW periods generally contribute a small fraction of PM (Wang et al., 2007;Vecchi et al., 2008). Therefore, our results suggest that burning of fireworks has the most impact on aerosol particles in the size range of 1 – 2.5 μm. Consistently, Vecchi et al. (2008) found the best correlation between the fireworks tracer, Sr, and the particles

255 between 700-800 nm (mobility diameter, D_m) which is approximately equivalent to
256 1.9 – 2.2 μm in D_{va} (vacuum aerodynamic diameter, D_{va}) with a density of 2.7 g cm^{-3}
257 (Zhang et al., 2010).

258 Figure 3 shows the average chemical composition of PM_1 and OA from
259 fireworks and also the background composition during LNY, LFD and LF. The
260 background PM_1 during LNY and LFD showed typical characteristics of clean
261 periods with high fraction of organics (> ~50%), whereas that during LF was
262 dominated by SIA (52%). As a comparison, organics constituted the major fraction of
263 FW-PM_1, contributing 44 – 55% on average. During LNY, FW exerted large impacts
264 on potassium and chloride whose contributions were elevated to 21% and 15% of
265 PM_1, respectively, from less than 7% (Chl) in the background aerosols. The large
266 increases of potassium and chloride were also observed during LFD and LF, and
267 previous studies in Beijing (Wang et al., 2007;Cheng et al., 2014). As shown in Fig. 3,
268 FW also emitted a considerable amount of sulfate, accounting for 7% - 14% of PM_1.
269 Sulfate correlated strongly with SO_2 during all three FW events (r^2 = 0.49 -0.92).
270 Given that the relative humidity was low, < 30% during LNY and LFD, and ~ 50%
271 during LF, aqueous-phase oxidation of SO_2 could not play significant roles for the
272 sulfate formation (Sun et al., 2013a). Therefore, sulfate in FW-PM_1 was mainly from
273 the direction emissions of FW. Compared to sulfate, FW appeared to show minor
274 impacts on nitrate, for example, 4% and 2% during LNY and LF, respectively.
275 Although nitrate contributed 12% of FW-PM_1 during LFD, most of it was likely from
276 local sources and/or regional transport as supported by the large contributions of local
277 HOA and COA in OA (Fig. 3b) and also a wind direction change in the middle.

278 The OOA contributed dominantly to OA during LNY, which is 79% on average

279 (Fig. 3a). As shown in Fig. 4, the mass spectrum of FW-organics is highly similar to
280 that of low-volatility OOA (LV-OOA, $r^2 = 0.94$; $r^2 = 0.89$ by excluding *m/z* 18 and 44)
281 (Ng et al., 2011a) indicating that the FW-organics is likely emitted in secondary.
282 Consistently, Drewnick et al. (2006) also found large enhancements of OOA-related
283 *m/z*'s (e.g., *m/z* 44) during New Year's fireworks, but HOA-related *m/z*'s (e.g., *m/z* 57)
284 are not significant contributors to FW organics. OOA contributed a much smaller
285 fraction of OA during LF (28%) due to the large contributions of POA components
286 (72%). Although the OOA contributions varied during three FW events, their absolute
287 concentrations were relatively close ranging from 5.8 to 7.9 μg m^{-3}. It should be noted
288 that our approach might overestimate the POA components in FW-OA because of the
289 influences of NFW sources, in particular during the FW period of LF when the local
290 HOA, COA, and CCOA happened to have large increases. By excluding the POA
291 components in FW-OA, FW on average contributed 15 – 19 μg m^{-3} PM_1 during three
292 FW events.

293 **3.3 Secondary aerosol and PM pollution**

294 The PM_1 (NR-PM_1 + BC) varied largely across the entire study with daily average
295 mass concentration ranging from 9.1 to 169 μg m^{-3}. The average PM_1 mass
296 concentration was 80 (±68) μg m^{-3}, which is approximately 20% higher than that
297 observed during winter 2011-2012 (Sun et al., 2013b). Organics composed the major
298 fraction of PM_1, accounting for 43%, followed by nitrate (22%), sulfate (14%),
299 ammonium (13%), BC (5%) and chloride (3%). The OA composition was dominated
300 by OOA (53%) with the rest being POA. Compared to winter 2011-2012 (Sun et al.,
301 2013b), this study showed significantly enhanced OOA (53% vs. 31%) and secondary
302 nitrate (22% vs. 16%), indicating that secondary formation have played important

303 roles in the formation of pollution episodes.

304 Figure 1d shows that submicron aerosol species alternated routinely between
305 pollution events (PEs) and clean periods (CPs) throughout the entire study. The PEs
306 generally lasted ~1 – 2 days except the one on 23 – 28 February that lasted more than
307 5 days, whereas the CPs were shorter, generally less than 1 day. In total, 9 PEs and 9
308 CPs were classified in this study (Fig. 1). A statistics of the mass concentrations and
309 mass fractions of aerosol species during the 9 PEs is presented in Fig. 5. The average
310 PM_1 mass concentration ranged 68 – 179 μg m^{-3} during PEs with the total secondary
311 particulate matter (SPM = OOA + SO_4^{2-} + NO_3^- +NH_4^+) accounting for 63 – 82%.
312 The average mass concentration of SPM for the 9 PEs was 86 (±32) μg m^{-3}, which is
313 nearly 3 times primary PM (PPM = HOA + COA +CCOA + BC + Chl) (30 ±9.5 μg
314 m^{-3}). SPM consistently dominated PM_1 across different PM levels (69 – 75%), but
315 generally with higher contributions (up to 81%) during daytime (Fig. 6b). The diurnal
316 cycle of SPM presented a gradual increase from 50 to 70 μg m^{-3} between 10:00 –
317 20:00, indicating evident photochemical production of secondary species during
318 daytime. It should be also noted that all secondary species showed ubiquitously higher
319 mass concentrations than those of primary species (Fig. 5a).

320 The SOA generally contributed more than 50% to OA with an average of 55%
321 during the PEs except the episode on 3 February (35%). It's interesting to note that
322 the contribution of POA increased as a function of organic loadings which varied
323 from ~35% to 63% when organics was above 80 μg m^{-3} (Fig. 6c). Such behavior is
324 mainly caused by the enhanced CCOA at high organic mass loadings, which was also
325 observed during winter 2011 – 2012 (Sun et al., 2013b). These results suggest that
326 POA played more important roles than SOA in PM pollution during periods with high

organic mass loadings. In fact, POA showed even higher concentrations than OOA at nighttime (0:00 – 8:00) due to the intensified local emissions, e.g., coal combustion for heating. Despite this, the role of POA in PM pollution was compensated by the elevated secondary inorganic species as a function of PM loadings (Fig. 6a) leading to the consistently dominant SPM across different pollution levels. Figure 7a shows an evidently lower contribution of organics to PM_1 during PEs than CPs. The elevated secondary inorganic species during PEs were closely related to the increase of RH (Fig. 1). For example, during the pollution episode on 3 February, the sulfate concentration increased rapidly and became the major inorganic species when RH was increased from ~60% to > 90%. The gaseous SO_2 showed a corresponding decrease indicating aqueous-phase processing of SO_2 to form sulfate, consistent with our previous conclusion that aqueous-phase processing could contribute more than 50% of sulfate production during winter 2011-2012 (Sun et al., 2013a).

The compositional differences between PEs and CPs also led to different mass extinction efficiency (MEE, 630 nm) of PM_1 (Fig. 7b). The higher MEE (6.4 m^2 g^{-1}) during PEs than CPs (4.4 m^2 g^{-1}) is primarily due to the enhanced secondary species, and also likely the increases of aerosol particle sizes although we don't have size data to support it. Similar increases of mass scattering efficiency from clean periods to relatively polluted conditions were also observed previously in Beijing and Shanghai (Jung et al., 2009;Huang et al., 2013). It should be noted that the MEE of PM_1 in this study refers to $PM_{2.5}$ b_{ext}/PM_1. If assuming PM_1 on average contributed 70% of $PM_{2.5}$, the real MEE of PM_1 during PEs and CPs would be 4.5 and 3.1 m^2 g^{-1}, respectively.

3.4 Holiday Effects on PM Pollution

Figure 8 shows a comparison of aerosol species, gaseous species, and

meteorological parameters between holiday (HD) and non-holiday (NHD) periods. The official holiday for the Spring Festival was 9 – 15 February. However, we noted a large decrease of cooking aerosols from 7 February until 19 February (Fig. S4c), whose emissions were expected to be stable under similar meteorological conditions. The decrease of COA was likely due to the reduction of the number of population in Beijing, which agreed with the fact that most migrants from outside Beijing were leaving for hometown before the official holiday. Therefore, 7 – 19 February was used as a longer holiday for a comparison. It was estimated that approximately half of population (9 million) left Beijing before Spring Festival (http://news.xinhuanet.com/yzyd/local/20130208/c_114658765.htm). Such a great reduction in human activities would exert a large impact on aerosol composition and sources in the city during holidays. To better investigate the HD effects on PM pollution, the data shown in Fig. 8 excluded the CPs marked in Fig. 1. The data with the CPs included are presented in Fig. S12.

The differences between HD and NHD for primary species varied largely among different species. COA showed the largest reduction (69%) among aerosol species with the average concentration decreasing from 5.8 μg m^{-3} during NHD to 1.8 μg m^{-3} during HD. The contribution of COA to OA showed a corresponding decrease from 12% to 4%. Given the similar meteorological conditions between HD and NHD, e.g., RH (46% vs. 52%) and wind speed (1.3 m s^{-1} vs. 1.2 m s^{-1}), the reduction of COA clearly indicated a large decrease of population and the number of restaurants open during HD. The CCOA showed approximately 30% reduction during HD, and its contribution to OA decreased from 23% to 18%. Not surprisingly, chloride showed a similar reduction as CCOA because it was primarily from coal combustion emissions

375 during wintertime (Sun et al., 2013b). Figure 8 also shows a significant reduction
376 (54%) for NO, indicating much less traffic emissions in the city during HD. The HOA,
377 however, even showed a slight increase during HD, which appeared to contradict with
378 the reduction of two combustion-related tracers, BC and CO (~20%). This can be
379 explained by the fact that coal combustion is a large source of BC and CO during
380 heating season (Tian et al., 2008;Zhi et al., 2008). Consistently, BC and CO showed
381 relatively similar reductions to CCOA. Therefore, the minor variations of HOA might
382 indicate that the number of heavy-duty vehicles and diesel trucks that dominated
383 HOA emissions (Massoli et al., 2012;Hayes et al., 2013) remained little change during
384 HD period although that of gasoline vehicles was largely decreased. It should be
385 noted that HOA showed a large peak on 9 February – the first day of the official
386 holiday (Fig. S4) when more traffic emissions were expected due to many people
387 leaving for hometown. After that, HOA showed slightly lower concentration during
388 11 – 17 February than other periods. In fact, the average HOA showed a slight
389 reduction (~5%) during the long holiday period (7 – 19 February) suggesting a small
390 holiday effect on HOA reduction. Together, the total primary aerosol species (PPM)
391 showed an average reduction of 22% because of holiday effects.

392 Nitrate showed the largest reduction among secondary species by 22% during HD,
393 primarily due to a reduction of its precursors NO and NO_2. Results here suggest that
394 reducing traffic emissions would help mitigate the nitrate pollution in the city.
395 Compared to nitrate, sulfate showed minor changes (2%) between HD and NHD, and
396 OOA even showed a slight increase (6%) during HD. One of the reasons is that
397 secondary sulfate and OOA were mainly formed over regional scale and less affected
398 by local production, consistent with their relatively flat diurnal cycles (Fig. S11).

Ammonium showed a reduction between nitrate and sulfate because ammonium mainly existed in the form of $(NH_4)_2SO_4$ and NH_4NO_3. Overall, secondary species showed generally lower reductions than primary species with the total secondary species (SPM) showing an average reduction of 9% during HD. The joint reductions of PPM and SPM led to an average reduction of 13% for PM_1 during HD. However, these reductions did not help alleviate the fine particle pollution during HD. The $PM_{2.5}$ excluding FW impacts even showed 27% increase from 96 μg m^{-3} during NHD to 122 μg m^{-3} during HD. The longer holiday (LHD, 7 – 19 February) showed similar influences on both primary and secondary species as the official holiday (9 – 15 February). COA, CCOA, and NO are the three species with the largest reductions during LHD (> 50%). However, HOA, SO_4^{2-}, OOA, and $PM_{2.5}$ showed rather small changes (< ±7%). Therefore, results in this study suggest that controlling the primary source emissions, e.g., cooking and traffic emissions in the city can reduce the primary particles largely, yet has limited effects on secondary species and the total fine particle mass. One of the reasons is that the severe PM pollution in Beijing is predominantly contributed by secondary species (see discussions above) that are formed over regional scales. Reducing the primary source emissions in local areas would have limited impacts on mitigation of air pollution in the city. Similarly, Guo et al. (2013) reported a large reduction of primary organic carbon (OC) from traffic emissions and coal combustion during the 2008 Olympic Summer Games when traffic restrictions and temporary closure of factories were implemented. However, secondary OC was not statistically different between controlled and non-controlled periods. Our results highlight the importance of implementing joint efforts over regional scales for air pollution control in north China.

4 Conclusions

We have characterized the aerosol particle composition and sources during the Chinese Spring Festival, 2013. The average PM_1 mass concentration was 80 (±68) μg m^{-3} for the entire study with organics being the major fraction (43%). Nine pollution events and nine clean periods with substantial compositional differences were observed. The secondary particulate matter (= SOA+ sulfate + nitrate + ammonium) played a dominant role for the PM pollution during the nine PEs. The contributions of SPM to PM_1 varied from 63% to 82% with SOA on average accounting for ~55% of OA. As a result, the average mass extinction efficiency of PM_1 during PEs (6.4 m^2 g^{-1}) was higher than that during CPs (4.4 m^2 g^{-1}). Three FW events, i.e., LNY, LFD, and LF, were identified, which showed significant and short-term impacts on fine particles, and non-refractory potassium, chloride, and sulfate in PM_1. The FW also exerted a large impact on organics that presented mainly in secondary as indicated by its similar mass spectrum to that of oxygenated OA. The holiday effects on aerosol composition and sources were also investigated by comparing the differences between holiday and non-holiday periods. The changes of anthropogenic source emissions during the holiday showed large impacts on reduction of cooking OA (69%), nitrogen monoxide (54%), and coal combustion OA (28%) in the city, yet presented minor influences on secondary species. The average SOA and the total $PM_{2.5}$ even increased slightly during the holiday period. Results here have significant implications that controlling the local primary source emissions, e.g., cooking and traffic activities, might have limited effects on improving air quality during polluted days when SPM dominated aerosol composition for most of time. Our results also highlight the importance of implementing joint measures over regional scales for mitigation of air pollution.

Acknowledgements

This work was supported by the National Key Project of Basic Research (2014CB447900), the Strategic Priority Research Program (B) of the Chinese Academy of Sciences (Grant No. XDB05020501), and the National Natural Science Foundation of China (41175108). We thank Huabin Dong, Hongyan Chen, and Zhe Wang's help in data collection, and also the Technical and Service Center, Institute of Atmospheric Physics, Chinese Academy of Sciences for providing meteorological data.

References

Chan, C. K., and Yao, X.: Air pollution in mega cities in China, Atmos. Environ., 42, 1-42, DOI: 10.1016/j.atmosenv.2007.09.003, 2008.

Cheng, Y., Engling, G., He, K.-b., Duan, F.-k., Du, Z.-y., Ma, Y.-l., Liang, L.-l., Lu, Z.-f., Liu, J.-m., Zheng, M., and Weber, R. J.: The characteristics of Beijing aerosol during two distinct episodes: Impacts of biomass burning and fireworks, Environ. Pollut., 185, 149-157, http://dx.doi.org/10.1016/j.envpol.2013.10.037, 2014.

DeCarlo, P. F., Kimmel, J. R., Trimborn, A., Northway, M. J., Jayne, J. T., Aiken, A. C., Gonin, M., Fuhrer, K., Horvath, T., Docherty, K. S., Worsnop, D. R., and Jimenez, J. L.: Field-Deployable, High-Resolution, Time-of-Flight Aerosol Mass Spectrometer, Anal. Chem., 78, 8281-8289, 2006.

Drewnick, F., Hings, S. S., Curtius, J., Eerdekens, G., and Williams, J.: Measurement of fine particulate and gas-phase species during the New Year's fireworks 2005 in Mainz, Germany, Atmos. Environ., 40, 4316-4327, 10.1016/j.atmosenv.2006.03.040, 2006.

Duan, F. K., He, K. B., Ma, Y. L., Yang, F. M., Yu, X. C., Cadle, S. H., Chan, T., and Mulawa, P. A.: Concentration and chemical characteristics of PM2.5 in Beijing, China: 2001–2002, Sci. Total Environ., 355, 264-275, 10.1016/j.scitotenv.2005.03.001, 2006.

Feng, J., Sun, P., Hu, X., Zhao, W., Wu, M., and Fu, J.: The chemical composition and sources of PM2.5 during the 2009 Chinese New Year's holiday in Shanghai, Atmospheric Research, 118, 435-444, http://dx.doi.org/10.1016/j.atmosres.2012.08.012, 2012.

Godri, K. J., Green, D. C., Fuller, G. W., Dall'Osto, M., Beddows, D. C., Kelly, F. J., Harrison, R. M., and Mudway, I. S.: Particulate oxidative burden associated with firework activity, 21, 8295-8301 pp., 2010.

Guo, S., Hu, M., Wang, Z. B., Slanina, J., and Zhao, Y. L.: Size-resolved aerosol water-soluble ionic compositions in the summer of Beijing: implication of regional secondary formation, Atmos. Chem. Phys., 10, 947-959, 10.5194/acp-10-947-2010, 2010.

Guo, S., Hu, M., Guo, Q., Zhang, X., Schauer, J. J., and Zhang, R.: Quantitative evaluation of emission controls on primary and secondary organic aerosol sources during Beijing 2008 Olympics, Atmos. Chem. Phys., 13, 8303-8314, 10.5194/acp-13-8303-2013, 2013.

Hayes, P. L., Ortega, A. M., Cubison, M. J., Froyd, K. D., Zhao, Y., Cliff, S. S., Hu, W. W., Toohey, D. W., Flynn, J. H., Lefer, B. L., Grossberg, N., Alvarez, S., Rappenglück, B., Taylor, J. W., Allan, J. D., Holloway, J. S., Gilman, J. B., Kuster, W. C., de Gouw, J. A., Massoli, P., Zhang, X., Liu, J., Weber, R. J., Corrigan, A. L., Russell, L. M., Isaacman, G., Worton, D. R., Kreisberg, N. M., Goldstein, A. H., Thalman, R., Waxman, E. M., Volkamer, R., Lin, Y. H., Surratt, J. D., Kleindienst, T. E., Offenberg, J. H., Dusanter, S., Griffith, S., Stevens, P. S., Brioude, J., Angevine, W. M., and Jimenez, J. L.: Organic aerosol composition and sources in Pasadena, California during the 2010 CalNex campaign, Journal of Geophysical Research: Atmospheres, 118, 9233–9257, 10.1002/jgrd.50530, 2013.

He, L.-Y., Huang, X.-F., Xue, L., Hu, M., Lin, Y., Zheng, J., Zhang, R., and Zhang, Y.-H.: Submicron aerosol analysis and organic source apportionment in an urban atmosphere in Pearl River Delta of China using high-resolution aerosol mass spectrometry, J. Geophys. Res., 116, D12304, 10.1029/2010jd014566, 2011.

Huang, K., Zhuang, G., Lin, Y., Wang, Q., Fu, J. S., Zhang, R., Li, J., Deng, C., and Fu, Q.: Impact of anthropogenic emission on air quality over a megacity – revealed from an intensive atmospheric campaign during the Chinese Spring Festival, Atmos. Chem. Phys., 12, 11631-11645, 10.5194/acp-12-11631-2012, 2012.

Huang, X. F., He, L. Y., Hu, M., Canagaratna, M. R., Sun, Y., Zhang, Q., Zhu, T., Xue, L., Zeng, L. W., Liu, X. G., Zhang, Y. H., Jayne, J. T., Ng, N. L., and Worsnop, D. R.: Highly time-resolved chemical characterization of atmospheric submicron particles during 2008 Beijing Olympic Games using an Aerodyne High-Resolution Aerosol Mass Spectrometer, Atmos. Chem. Phys., 10, 8933-8945, 10.5194/acp-10-8933-2010, 2010.

Huang, Y., Li, L., Li, J., Wang, X., Chen, H., Chen, J., Yang, X., Gross, D. S., Wang, H., Qiao, L., and Chen, C.: A case study of the highly time-resolved evolution of aerosol chemical and optical properties in urban Shanghai, China, Atmos. Chem. Phys., 13, 3931-3944, 10.5194/acp-13-3931-2013, 2013.

Jayne, J. T., Leard, D. C., Zhang, X., Davidovits, P., Smith, K. A., Kolb, C. E., and Worsnop, D. R.: Development of an aerosol mass spectrometer for size and composition analysis of submicron particles, Aerosol Sci. Tech., 33, 49-70, 2000.

524 Jung, J., Lee, H., Kim, Y. J., Liu, X., Zhang, Y., Hu, M., and Sugimoto, N.: Optical
525 properties of atmospheric aerosols obtained by in situ and remote measurements
526 during 2006 Campaign of Air Quality Research in Beijing (CAREBeijing-2006), J.
527 Geophys. Res., 114, D00G02, 10.1029/2008jd010337, 2009.
528 Li, W., Shi, Z., Yan, C., Yang, L., Dong, C., and Wang, W.: Individual metal-bearing
529 particles in a regional haze caused by firecracker and firework emissions, Sci.
530 Total Environ., 443, 464-469, http://dx.doi.org/10.1016/j.scitotenv.2012.10.109,
531 2013.
532 Massoli, P., Kebabian, P. L., Onasch, T. B., Hills, F. B., and Freedman, A.: Aerosol
533 Light Extinction Measurements by Cavity Attenuated Phase Shift (CAPS)
534 Spectroscopy: Laboratory Validation and Field Deployment of a Compact Aerosol
535 Particle Extinction Monitor, Aerosol Sci. Tech., 44, 428-435,
536 10.1080/02786821003716599, 2010.
537 Massoli, P., Fortner, E. C., Canagaratna, M. R., Williams, L. R., Zhang, Q., Sun, Y.,
538 Schwab, J. J., Trimborn, A., Onasch, T. B., Demerjian, K. L., Kolb, C. E.,
539 Worsnop, D. R., and Jayne, J. T.: Pollution Gradients and Chemical
540 Characterization of Particulate Matter from Vehicular Traffic Near Major
541 Roadways: Results from the 2009 Queens College Air Quality Study in NYC,
542 Aerosol Sci. Tech., 46, 1201-1218, 10.1080/02786826.2012.701784, 2012.
543 Matthew, B. M., Middlebrook, A. M., and Onasch, T. B.: Collection Efficiencies in an
544 Aerodyne Aerosol Mass Spectrometer as a Function of Particle Phase for
545 Laboratory Generated Aerosols, Aerosol Sci. Tech., 42, 884 - 898, 2008.
546 Middlebrook, A. M., Bahreini, R., Jimenez, J. L., and Canagaratna, M. R.: Evaluation
547 of Composition-Dependent Collection Efficiencies for the Aerodyne Aerosol
548 Mass Spectrometer using Field Data, Aerosol Sci. Tech., 46, 258-271, 2012.
549 Molina, M. J., and Molina, L. T.: Megacities and atmospheric pollution, J. Air Waste
550 Manage. Assoc., 54, 644–680, 2004.
551 Moreno, T., Querol, X., Alastuey, A., Cruz Minguillón, M., Pey, J., Rodriguez, S.,
552 Vicente Miró, J., Felis, C., and Gibbons, W.: Recreational atmospheric pollution
553 episodes: Inhalable metalliferous particles from firework displays, Atmos.
554 Environ., 41, 913-922, http://dx.doi.org/10.1016/j.atmosenv.2006.09.019, 2007.
555 Ng, N. L., Canagaratna, M. R., Jimenez, J. L., Zhang, Q., Ulbrich, I. M., and Worsnop,
556 D. R.: Real-Time Methods for Estimating Organic Component Mass
557 Concentrations from Aerosol Mass Spectrometer Data, Environ. Sci. Technol., 45,
558 910-916, 10.1021/es102951k, 2011a.
559 Ng, N. L., Herndon, S. C., Trimborn, A., Canagaratna, M. R., Croteau, P. L., Onasch,
560 T. B., Sueper, D., Worsnop, D. R., Zhang, Q., Sun, Y. L., and Jayne, J. T.: An
561 Aerosol Chemical Speciation Monitor (ACSM) for Routine Monitoring of the
562 Composition and Mass Concentrations of Ambient Aerosol, Aerosol Sci. Tech.,
563 45, 770 - 784, 2011b.
564 Paatero, P., and Tapper, U.: Positive matrix factorization: A non-negative factor
565 model with optimal utilization of error estimates of data values, Environmetrics, 5,
566 111-126, 1994.

Slowik, J. G., Stroud, C., Bottenheim, J. W., Brickell, P. C., Chang, R. Y. W., Liggio, J., Makar, P. A., Martin, R. V., Moran, M. D., Shantz, N. C., Sjostedt, S. J., van Donkelaar, A., Vlasenko, A., Wiebe, H. A., Xia, A. G., Zhang, J., Leaitch, W. R., and Abbatt, J. P. D.: Characterization of a large biogenic secondary organic aerosol event from eastern Canadian forests, Atmos. Chem. Phys., 10, 2825-2845, 2010.

Song, Y., Zhang, Y., Xie, S., Zeng, L., Zheng, M., Salmon, L. G., Shao, M., and Slanina, S.: Source apportionment of PM2.5 in Beijing by positive matrix factorization, Atmos. Environ., 40, 1526-1537, DOI: 10.1016/j.atmosenv.2005.10.039, 2006.

Sun, J., Zhang, Q., Canagaratna, M. R., Zhang, Y., Ng, N. L., Sun, Y., Jayne, J. T., Zhang, X., Zhang, X., and Worsnop, D. R.: Highly time- and size-resolved characterization of submicron aerosol particles in Beijing using an Aerodyne Aerosol Mass Spectrometer, Atmos. Environ., 44, 131-140, 2010.

Sun, Y., Zhuang, G., Tang, A., Wang, Y., and An, Z.: Chemical Characteristics of $PM_{2.5}$ and PM_{10} in Haze-Fog Episodes in Beijing, Environ. Sci. Technol., 40, 3148-3155, 2006.

Sun, Y. L., Wang, Z., Dong, H., Yang, T., Li, J., Pan, X., Chen, P., and Jayne, J. T.: Characterization of summer organic and inorganic aerosols in Beijing, China with an Aerosol Chemical Speciation Monitor, Atmos. Environ., 51, 250-259, 10.1016/j.atmosenv.2012.01.013, 2012.

Sun, Y. L., Wang, Z., Fu, P., Jiang, Q., Yang, T., Li, J., and Ge, X.: The Impact of Relative Humidity on Aerosol Composition and Evolution Processes during Wintertime in Beijing, China, Atmos. Environ., 77, 927–934, http://dx.doi.org/10.1016/j.atmosenv.2013.06.019, 2013a.

Sun, Y. L., Wang, Z. F., Fu, P. Q., Yang, T., Jiang, Q., Dong, H. B., Li, J., and Jia, J. J.: Aerosol composition, sources and processes during wintertime in Beijing, China, Atmos. Chem. Phys., 13, 4577-4592, 10.5194/acp-13-4577-2013, 2013b.

Tian, L., Lucas, D., Fischer, S. L., Lee, S. C., Hammond, S. K., and Koshland, C. P.: Particle and Gas Emissions from a Simulated Coal-Burning Household Fire Pit, Environ. Sci. Technol., 42, 2503-2508, 10.1021/es0716610, 2008.

Ulbrich, I. M., Canagaratna, M. R., Zhang, Q., Worsnop, D. R., and Jimenez, J. L.: Interpretation of organic components from Positive Matrix Factorization of aerosol mass spectrometric data, Atmos. Chem. Phys., 9, 2891-2918, 2009.

Vecchi, R., Bernardoni, V., Cricchio, D., D'Alessandro, A., Fermo, P., Lucarelli, F., Nava, S., Piazzalunga, A., and Valli, G.: The impact of fireworks on airborne particles, Atmos. Environ., 42, 1121-1132, 10.1016/j.atmosenv.2007.10.047, 2008.

Wang, Y., Zhuang, G., Sun, Y., and An, Z.: The variation of characteristics and formation mechanisms of aerosols in dust, haze, and clear days in Beijing, Atmos. Environ., 40, 6579-6591, 2006.

608 Wang, Y., Zhuang, G., Xu, C., and An, Z.: The air pollution caused by the burning of
609 fireworks during the lantern festival in Beijing, Atmos. Environ., 41, 417-431,
610 10.1016/j.atmosenv.2006.07.043, 2007.
611 Yang, F., Tan, J., Zhao, Q., Du, Z., He, K., Ma, Y., Duan, F., and Chen, G.:
612 Characteristics of PM2.5 speciation in representative megacities and across China,
613 Atmos. Chem. Phys., 11, 5207-5219, 10.5194/acp-11-5207-2011, 2011.
614 Yang, L., Gao, X., Wang, X., Nie, W., Wang, J., Gao, R., Xu, P., Shou, Y., Zhang, Q.,
615 and Wang, W.: Impacts of firecracker burning on aerosol chemical characteristics
616 and human health risk levels during the Chinese New Year Celebration in Jinan,
617 China, Sci. Total Environ., 476–477, 57-64,
618 http://dx.doi.org/10.1016/j.scitotenv.2013.12.110, 2014.
619 Yao, X., Chan, C. K., Fang, M., Cadle, S., Chan, T., Mulawa, P., He, K., and Ye, B.:
620 The water-soluble ionic composition of PM2.5 in Shanghai and Beijing, China,
621 Atmos. Environ., 36, 4223-4234, Doi: 10.1016/s1352-2310(02)00342-4, 2002.
622 Zhang, J. K., Sun, Y., Liu, Z. R., Ji, D. S., Hu, B., Liu, Q., and Wang, Y. S.:
623 Characterization of submicron aerosols during a month of serious pollution in
624 Beijing, 2013, Atmos. Chem. Phys., 14, 2887-2903, 10.5194/acp-14-2887-2014,
625 2014.
626 Zhang, M., Wang, X., Chen, J., Cheng, T., Wang, T., Yang, X., Gong, Y., Geng, F.,
627 and Chen, C.: Physical characterization of aerosol particles during the Chinese
628 New Year's firework events, Atmos. Environ., 44, 5191-5198,
629 10.1016/j.atmosenv.2010.08.048, 2010.
630 Zhang, Q., Jimenez, J., Canagaratna, M., Ulbrich, I., Ng, N., Worsnop, D., and Sun,
631 Y.: Understanding atmospheric organic aerosols via factor analysis of aerosol
632 mass spectrometry: a review, Anal. Bioanal. Chem., 401, 3045-3067,
633 10.1007/s00216-011-5355-y, 2011.
634 Zhang, R., Jing, J., Tao, J., Hsu, S. C., Wang, G., Cao, J., Lee, C. S. L., Zhu, L., Chen,
635 Z., Zhao, Y., and Shen, Z.: Chemical characterization and source apportionment
636 of PM2.5 in Beijing: seasonal perspective, Atmos. Chem. Phys., 13, 7053-7074,
637 10.5194/acp-13-7053-2013, 2013.
638 Zhao, S., Yu, Y., Yin, D., Liu, N., and He, J.: Ambient particulate pollution during
639 Chinese Spring Festival in urban Lanzhou, Northwestern China, Atmospheric
640 Pollution Research, 5, 335-343, doi: 10.5094/APR.2014.039, 2014.
641 Zhao, X. J., Zhao, P. S., Xu, J., Meng, W., Pu, W. W., Dong, F., He, D., and Shi, Q.
642 F.: Analysis of a winter regional haze event and its formation mechanism in the
643 North China Plain, Atmos. Chem. Phys., 13, 5685-5696,
644 10.5194/acp-13-5685-2013, 2013.
645 Zheng, M., Salmon, L. G., Schauer, J. J., Zeng, L., Kiang, C. S., Zhang, Y., and Cass,
646 G. R.: Seasonal trends in PM2.5 source contributions in Beijing, China, Atmos.
647 Environ., 39, 3967-3976, DOI: 10.1016/j.atmosenv.2005.03.036, 2005.
648 Zhi, G., Chen, Y., Feng, Y., Xiong, S., Li, J., Zhang, G., Sheng, G., and Fu, J.:
649 Emission characteristics of carbonaceous particles from various residential
650 coal-stoves in China, Environ. Sci. Technol., 42, 3310-3315, 2008.

Figure Captions:

Fig. 1. Time series of meteorological parameters (a) relative humidity (RH) and temperature (T); (b) wind direction (WD) and wind speed (WS) at the height of 100 m; mass concentrations of (c) $PM_{2.5}$ and NR-PM_1 + BC and (d) submicron aerosol species. Also shown in (a) and (b) is the temperature and wind speed at the height of 8 m which are in blue. The extinction coefficient (b_{ext}) at 630 nm is shown in (c). Three events, i.e., Lunar New Year (LNY), Lunar Fifth Day (LFD) and Lantern Festival (LF) with significant influences of fireworks are marked in (c). In addition, the classified clean periods (CPs) and polluted events (PEs) are marked as shaded light blue and pink areas, respectively. A more detailed time series of aerosol species during the three fireworks events are shown in Fig. S9.

Fig. 2. Correlation of PM_1 vs. $PM_{2.5}$ with the data segregated into three fireworks events (LNY, LFD, and LF) and non-fireworks periods (NFW). The blank circles represent FW data between 18:00 – 23:30 on 9 February which had large influences from NFW sources.

Fig. 3. Average chemical composition of PM_1 and OA from fireworks and background during three FW events.

Fig. 4. (a) Average mass spectra (MS) of OA during the firework period of Lunar New Year (23:30, 9 February – 3:30, 10 February) and the period of background (BG, 4:30 – 11:00, 10 February). (b) Comparison of the difference spectrum from (a), i.e., $MS_{FW+BG} - MS_{BG}$, with the average LV-OOA spectrum in Ng et al.(2011a). Five *m/z*'s, 37 ($^{37}Cl^+$), 58 ($NaCl^+$), 60 ($Na^{37}Cl^+$), 74 (KCl^+), and 76 ($K^{37}Cl^+$/ $^{41}KCl^+$) with significant influences of fireworks are marked.

Fig. 5. Box plots of (a) mass concentrations and (b) mass fractions of aerosol species for 9 pollution events marked in Fig. 1. The mean (cross), median (horizontal line), 25th and 75th percentiles (lower and upper box), and 10th and 90th percentiles (lower and upper whiskers) are shown for each box.

Fig. 6. Left: variations of chemical composition of (a) organics, SNA (=sulfate + nitrate + ammonium), and others (the rest species in PM_1); (b) SPM and PPM; and (c) SOA and POA as a function of PM_1 and organics loadings, respectively. Right panels show their corresponding diurnal compositions.

Fig. 7. (a) Average mass fraction of organics (f_{Org}) as a function of PM_1 mass, and (b) correlations of extinction coefficients ($PM_{2.5}$) vs. PM_1 for 9 pollution events (PEs) and 9 clean periods (CPs) marked in Fig. 1. The error bar represents one standard deviations of the average for each event.

Fig. 8. The average ratios of aerosol species, gaseous species, PM mass concentrations, extinction coefficient, and meteorological parameters between holiday (HD) and non-holiday (NHD) periods. Two different holidays, i.e., the official holiday of 9 – 15 February and the longer holiday of 7 – 20 February were used for averages. Also note that the averages were made by excluding clean periods and firework events during both HD and NHD days.

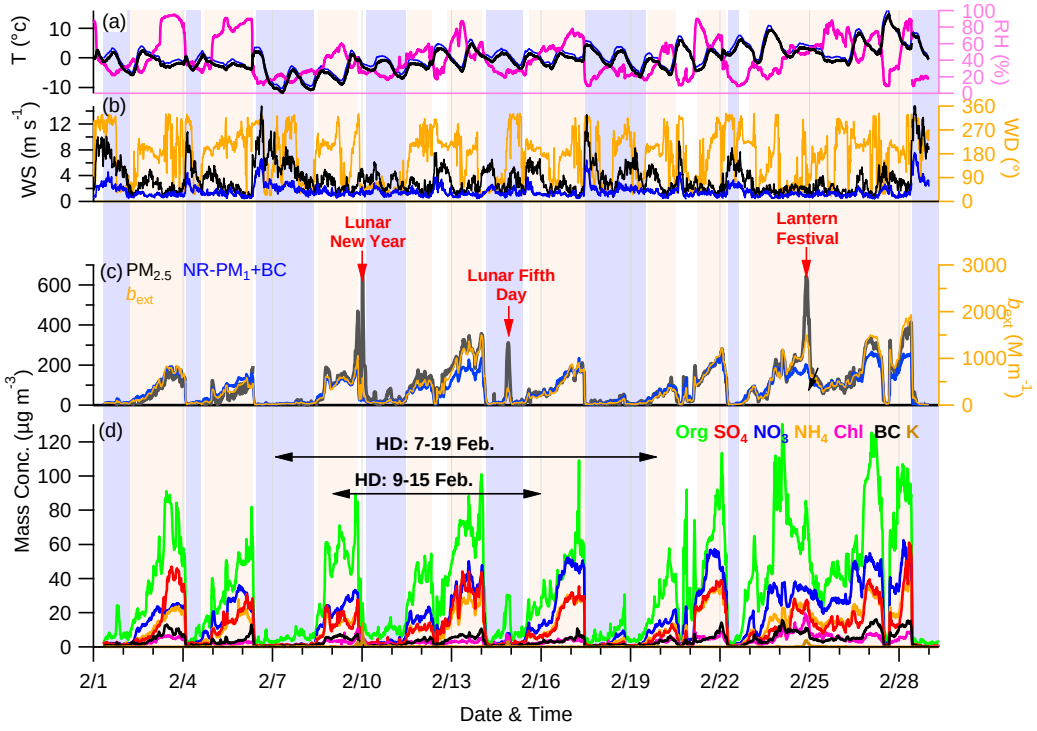

692

693 **Fig. 1.** Time series of meteorological parameters (a) relative humidity (RH) and
694 temperature (T); (b) wind direction (WD) and wind speed (WS) at the height of 100 m;
695 mass concentrations of (c) $PM_{2.5}$ and NR-PM_1 + BC and (d) submicron aerosol
696 species. Also shown in (a) and (b) is the temperature and wind speed at the height of 8
697 m which are in blue. The extinction coefficient (b_{ext}) at 630 nm is shown in (c). Three
698 events, i.e., Lunar New Year (LNY), Lunar Fifth Day (LFD) and Lantern Festival (LF)
699 with significant influences of fireworks are marked in (c). In addition, the classified
700 clean periods (CPs) and polluted events (PEs) are marked as shaded light blue and
701 pink areas, respectively. A more detailed time series of aerosol species during the
702 three fireworks events are shown in Fig. S9.

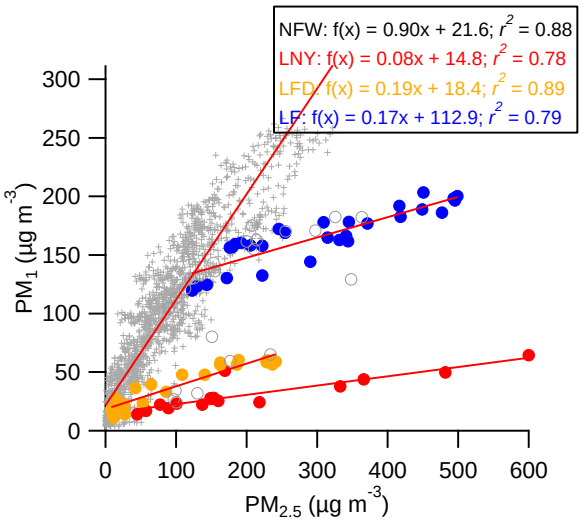

703

704 **Fig. 2.** Correlation of PM_1 vs. $PM_{2.5}$ with the data segregated into three fireworks
705 events (LNY, LFD, and LF) and non-fireworks periods (NFW). The blank circles
706 represent FW data between 18:00 – 23:30 on 9 February which had large influences
707 from NFW sources.

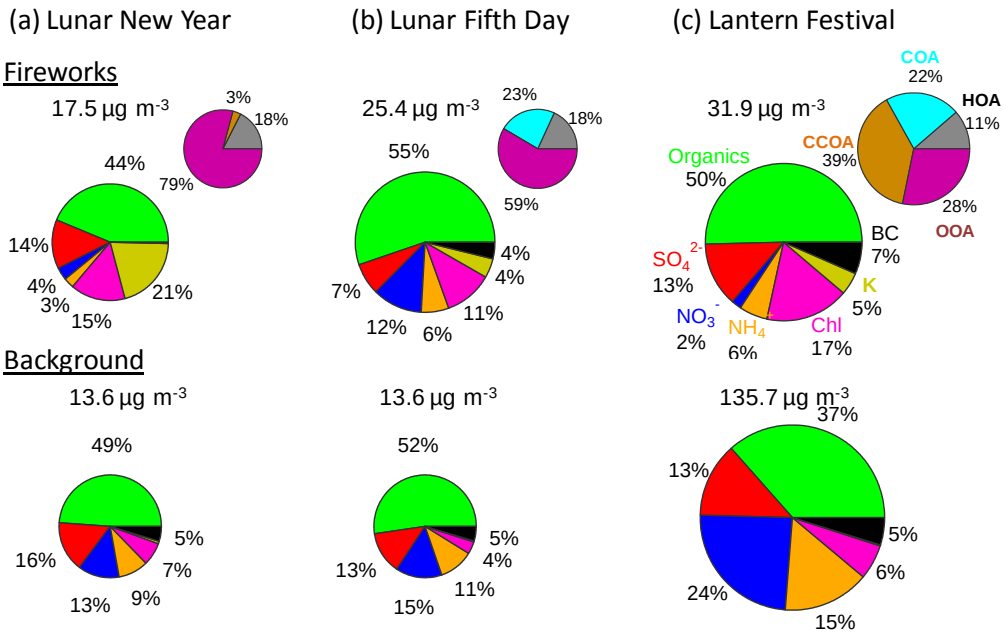

708

709 **Fig. 3.** Average chemical composition of PM_1 and OA from fireworks and
710 background during three FW events.

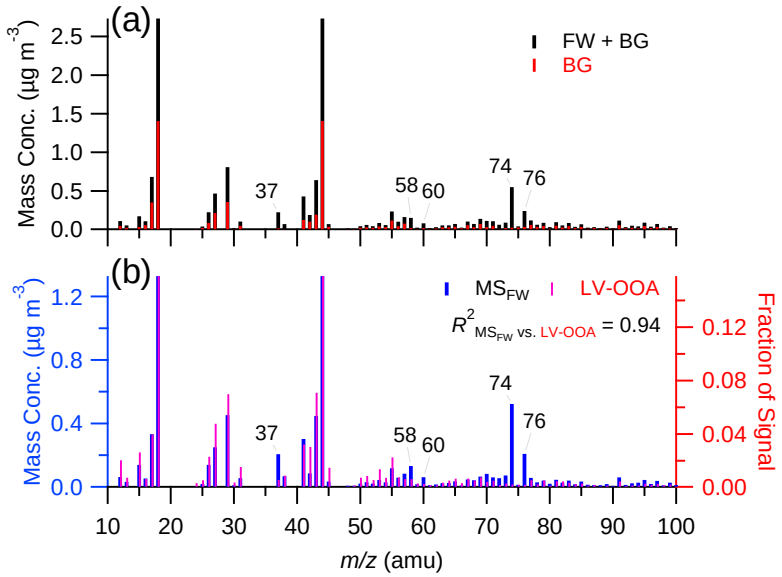

711

712 **Fig. 4.** (a) Average mass spectra (MS) of OA during the firework period of Lunar
713 New Year (23:30, 9 February – 3:30, 10 February) and the period of background (BG,
714 4:30 – 11:00, 10 February). (b) Comparison of the difference spectrum from (a), i.e.,
715 $MS_{FW+BG} - MS_{BG}$, with the average LV-OOA spectrum in Ng et al.(2011a). Five
716 *m/z*'s, 37 ($^{37}Cl^+$), 58 ($NaCl^+$), 60 ($Na^{37}Cl^+$), 74 (KCl^+), and 76 ($K^{37}Cl^+$/ $^{41}KCl^+$) with
717 significant influences of fireworks are marked.

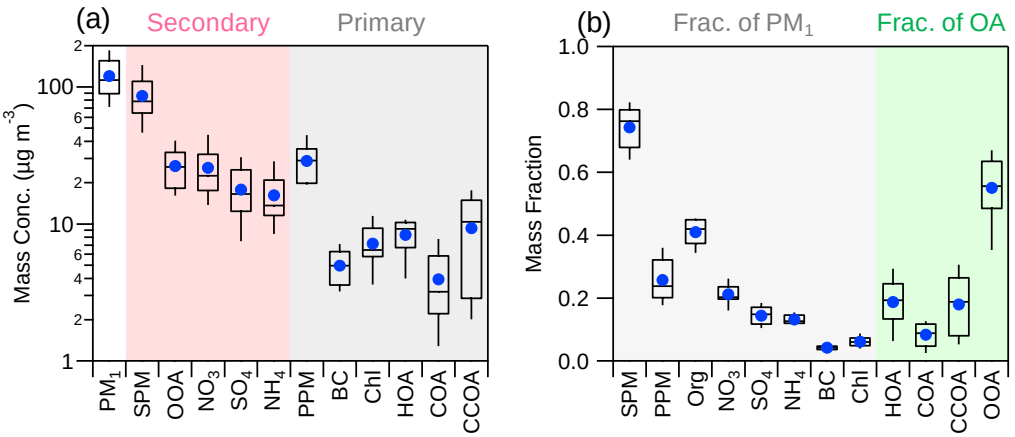

718

719 **Fig. 5.** Box plots of (a) mass concentrations and (b) mass fractions of aerosol species
720 for 9 pollution events marked in Fig. 1. The mean (cross), median (horizontal line),
721 25th and 75th percentiles (lower and upper box), and 10th and 90th percentiles (lower
722 and upper whiskers) are shown for each box.

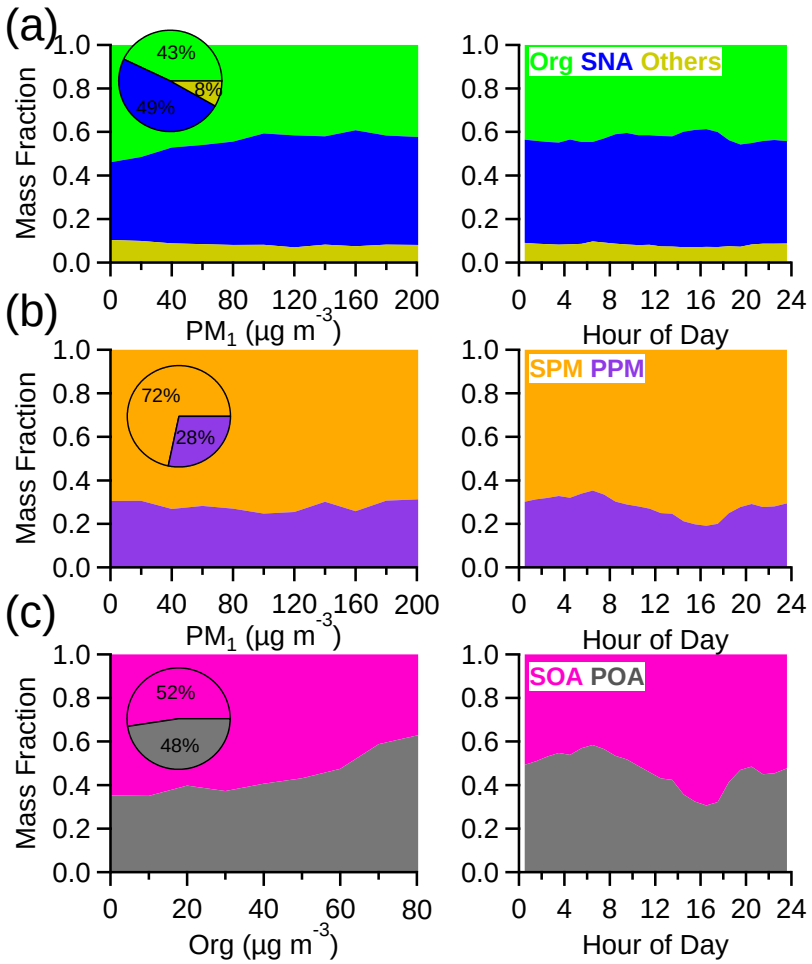

723

724 **Fig. 6.** Left: variations of chemical composition of (a) organics, SNA (=sulfate +
725 nitrate + ammonium), and others (the rest species in PM_1); (b) SPM and PPM; and (c)
726 SOA and POA as a function of PM_1 and organics loadings, respectively. Right panels
727 show their corresponding diurnal compositions.

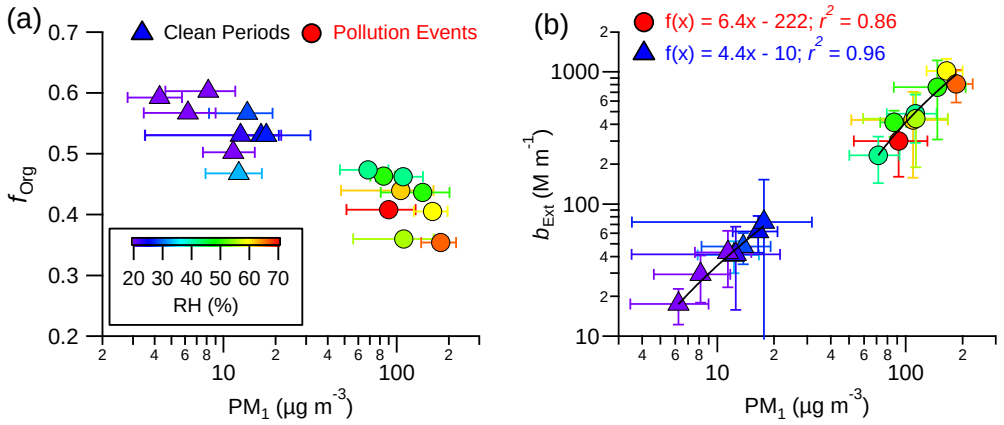

728

729 **Fig. 7.** (a) Average mass fraction of organics (f_{Org}) as a function of PM_1 mass, and (b)
730 correlations of extinction coefficients ($PM_{2.5}$) vs. PM_1 for 9 pollution events (PEs) and
731 9 clean periods (CPs) marked in Fig. 1. The error bar represents one standard
732 deviations of the average for each event.

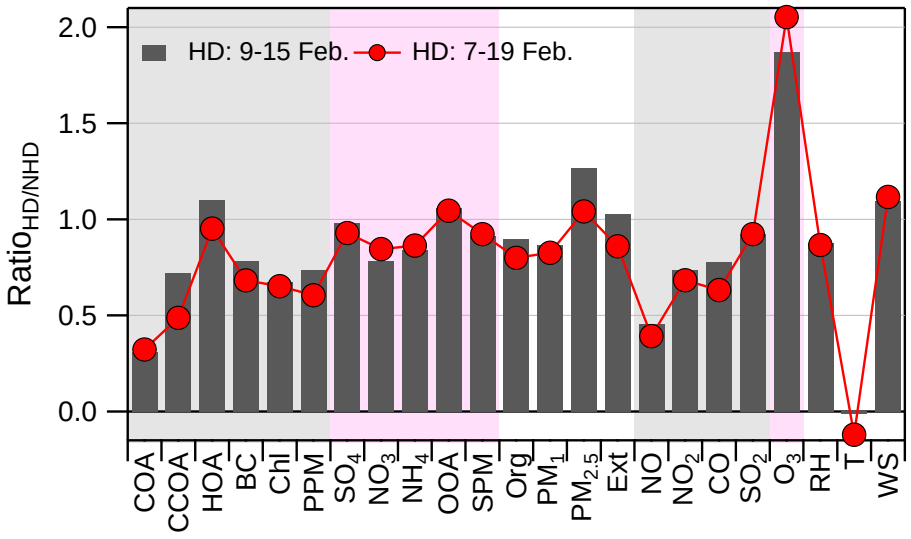

733

734 **Fig. 8.** The average ratios of aerosol species, gaseous species, PM mass
735 concentrations, extinction coefficient, and meteorological parameters between holiday
736 (HD) and non-holiday (NHD) periods. Two different holidays, i.e., the official
737 holiday of 9 – 15 February and the longer holiday of 7 – 20 February were used for
738 averages. Also note that the averages were made by excluding clean periods and
739 firework events during both HD and NHD days.